Master Thesis

Julia Ribbrock

Modeling and flow control for a left ventricular assist device

CHAIR FOR MEDICAL INFORMATION TECHNOLOGY
Faculty of Electrical Engineering and Information Technology, RWTH Aachen
Univ.-Prof. Dr.-Ing. Dr. med. Dr. h.c. Steffen Leonhardt
Supervisor: Patrick Borchers, M.Sc.
Date: December 21, 2020

Eidesstattliche Versicherung

Name, Vorname

Matrikelnummer (freiwillige Angabe)

Ich versichere hiermit an Eides Statt, dass ich die vorliegende Arbeit/Bachelorarbeit/ Masterarbeit* mit dem Titel

selbständig und ohne unzulässige fremde Hilfe erbracht habe. Ich habe keine anderen als die angegebenen Quellen und Hilfsmittel benutzt. Für den Fall, dass die Arbeit zusätzlich auf einem Datenträger eingereicht wird, erkläre ich, dass die schriftliche und die elektronische Form vollständig übereinstimmen. Die Arbeit hat in gleicher oder ähnlicher Form noch keiner Prüfungsbehörde vorgelegen.

Ort, Datum

Unterschrift

*Nichtzutreffendes bitte streichen

Belehrung:

§ 156 StGB: Falsche Versicherung an Eides Statt

Wer vor einer zur Abnahme einer Versicherung an Eides Statt zuständigen Behörde eine solche Versicherung falsch abgibt oder unter Berufung auf eine solche Versicherung falsch aussagt, wird mit Freiheitsstrafe bis zu drei Jahren oder mit Geldstrafe bestraft.

§ 161 StGB: Fahrlässiger Falscheid; fahrlässige falsche Versicherung an Eides Statt

(1) Wenn eine der in den §§ 154 bis 156 bezeichneten Handlungen aus Fahrlässigkeit begangen worden ist, so tritt Freiheitsstrafe bis zu einem Jahr oder Geldstrafe ein.

(2) Straflosigkeit tritt ein, wenn der Täter die falsche Angabe rechtzeitig berichtigt. Die Vorschriften des § 158 Abs. 2 und 3 gelten entsprechend.

Die vorstehende Belehrung habe ich zur Kenntnis genommen:

Ort, Datum

Unterschrift

Abstract

Contents

List of Figures

List of Tables

List of Symbols

Abbreviations

A-V valve	Atrioventricular valve
BTD	Bridging to decision
BTR	Bridging to recovery
BTT	Bridging to transplantation
BVAD	Biventricular Assist Device
CHR	Chien Hrones Reswick
CO	Cardiac Output
CVDs	Cardiovascular Diseases
CVS	Cardiovascular System
DT	Destination therapy
EDV	End-diastolic volume
EF	Ejection fraction
ESV	End-systolic volume
HiL	Hardware in the Loop
HR	Heart rate
HTx	Heart transplantation
ILC	Iterative learning control
IMACS	International Mechanically Assisted Circulatory Support
INTERMACS	Interagency Registry for Mechanically Assisted Circulatory Support
LVAD	Left Ventricular Assist Device
MCL	Mock circulatory loop
MCS	Mechanical Circulatory Support
RWTH Aachen	Rheinisch-Westfälische Technische Hochschule Aachen
SL valve	Semilunar valve
SV	Stroke Volume
VADs	Ventricular Assist Devices
WHO	World Health Organization
ZN	Ziegler Nichols

1 Introduction

1.1 Motivation and goal

1.2 Thesis structure

2 Medical Fundamentals

An important prerequisite to the work addressed in this thesis, is comprehension of the physiology of the human heart and the cardiovascular system. Therefore, the theoretical foundations of these topics will be introduced in this chapter.

2.1 Cardiovascular System

The fundamental task of the cardiovascular system is to supply all organs with blood through circulation. The human cardiovascular system is divided into two components, the systemic circulation and the pulmonary circulation. The systemic circulation is supplying blood flow to all tissues and organs apart from the lungs. Figure 2.1 represents the distribution of the blood over the circulatory system. [Hal16]

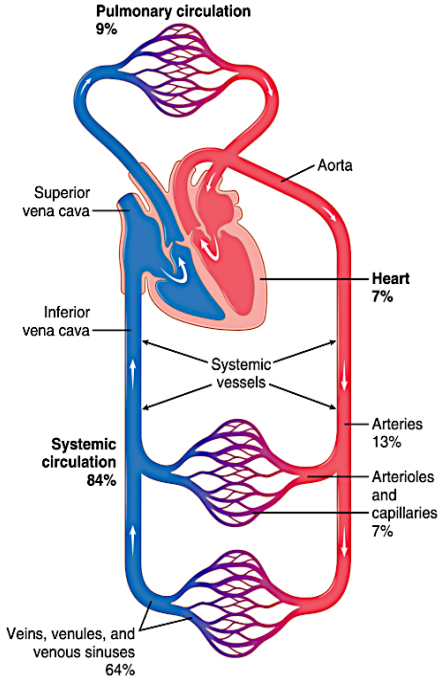

Figure 2.1: Blood distribution in the circulatory system [Hal16]. Red highlighting representing oxygenated, blue highlighting depicting deoxygenated blood flow.

The center of the cardiovascular system is the heart. The heart itself consists of two mechanical pumps, which are functionally connected in series but are united in one organ. It is separated into two sides, which themselves are divided into an atrium and

a ventricle each. The atria act as weak primer pumps needed to provide blood flow to the ventricles. [SLH11] Both, the atria and the ventricles are surrounded by the myocardium, which serves as the working muscle of the heart. Through contraction of the myocardium, blood is pumped into the circulatory system. [SK07] The left ventricle is pumping oxygenated blood through the aorta into the systemic circulation. There, the oxygen stored in the blood is delivered to the organs. The blood, now low in oxygen, is then led into the right atrium through the inferior and superior vena cava. From the right atrium, the deoxygenated blood then enters the right ventricle. Afterwards it is directed into the pulmonary circulation via the pulmonary artery. When the blood is oxygenated in the lungs, it is returned to the left atrium through the pulmonary vein. [SLH11] In addition to the atria and the ventricles each side of the heart has an atrioventricular (A-V) valve, as well as a semilunar (SL) valve. The A-V valve of the left heart is called the mitral valve, the one of the right heart is referred to as the tricuspid valve. The aortic valve and pulmonary valve are the SL valves of the left and right heart, respectively. The valves determine the direction of blood flow and thus prevent backflow. [SK07] A graphic overview of the anatomy and the course of blood flow through the heart is provided by Figure 2.2.

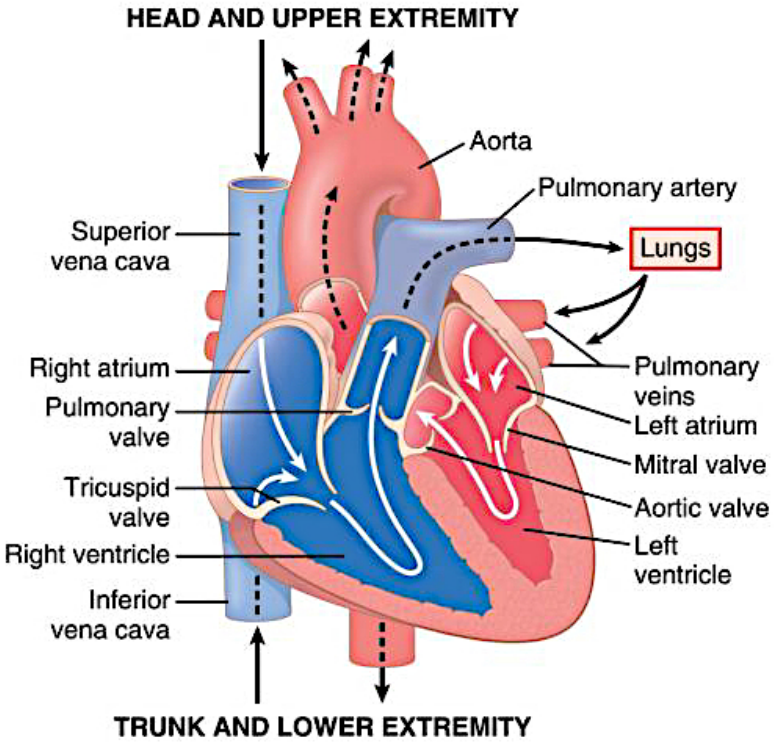

Figure 2.2: Anatomy of the human heart [Hal16]. Red highlighting representing oxygenated, blue highlighting depicting deoxygenated blood flow.

The amount of blood pumped through both sides of the heart, called cardiac output (CO), is equal at all times. It is determined by multiplying the heart rate (HR) and the stroke volume (SV). For an average adult at rest, with a heart rate of approximately $70\,min^{-1}$ and a stroke volume of $70\,ml$, this leads to

$$CO = HR \times SV = 70\,min^{-1} \times 70\,ml = 5\,\frac{l}{min}. \tag{2.1}$$

In case of maximum physical load, given at a stroke volume of $110\,ml$ and a heart rate of $190\,min^{-1}$, the cardiac output, as defined by (2.1), can increase to up to $20\,\frac{l}{min}$. [SLH11]

The cardiac cycle comprises the events that occur during the time-span of one heartbeat. It is triggered by an electrochemical action potential originating from the sinus node. The cycle is divided into four phases. Figure 2.3 illustrates these action phases and events of the cardiac cycle for the left ventricle. During the period of isovolumic

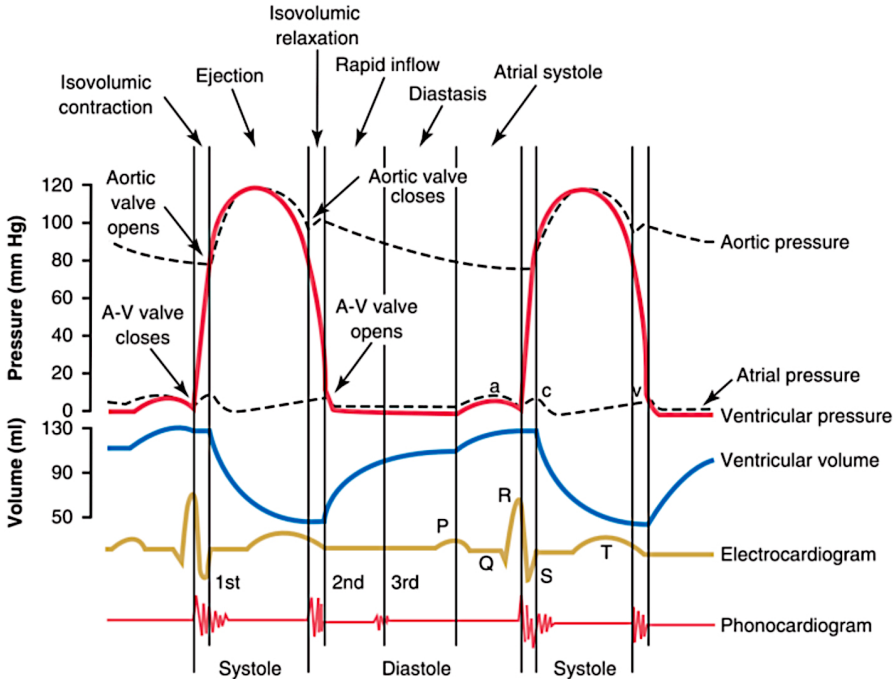

Figure 2.3: Action phases of the cardiac cycle based on the example of the left ventricle [Hal16].

contraction, the ventricular pressure increases. For the left ventricle, the pressure increases from about $4 - 6\,mmHg$ to $80\,mmHg$, whilst the pressure values for the right ventricle are much lower. This increase is occuring as a direct result of the ventricular contraction. The A-V valves, as well as the SL valves, are closed during

this process, leading to a constant blood volume in the ventricles. As soon as the ventricular pressure exceeds the arterial pressure, the pulmonary and aortic valves open and blood can flow into the aorta and the pulmonary artery. This phase is called ejection phase, as the blood is ejected into the circulatory system. The period of isovolumic contraction combined with the ejection phase comprises the ventricular systole. [SLH11] During the systole the blood volume in the ventricle decreases by $55 - 60\,\%$, resulting in an end-systolic volume (ESV) of about $40 - 50\,ml$ [Hal16]. Due to the contraction of the myocardium, the ventricular pressure keeps increasing for a while before decreasing again as relaxation of the myocardium sets in. As soon as the outflow of blood ends, the semilunar valves close, initiating the period of isovolumic relaxation. During this period pressure in the ventricles is decreasing, while blood volume is constant. When the pressure in the atrium exceeds the ventricular pressure, the A-V valves open. This leads to blood flowing into the ventricles until pressure levels in the atria and ventricles are equalized. [SLH11] This phase is referred to as period of rapid filling of the ventricles. Combined with the isovolumic relaxation it represents the diastole. The end-diastolic volume (EDV) is about $110 - 120\,ml$. [Hal16] While, at rest, the diastole lasts about twice as long as the systole, above a heart rate of $150\,min^{-1}$, the two phases are about equal [SLH11].

The pumping mechanism of the left ventricle can be illustrated well using a pressure-volume diagram (P-V diagram). Construction of the P-V diagram requires discussing the relationship between the left ventricular volume and the ventricular pressure during diastole and systole, as displayed in Figure 2.4a, first. Figure 2.4a displays to

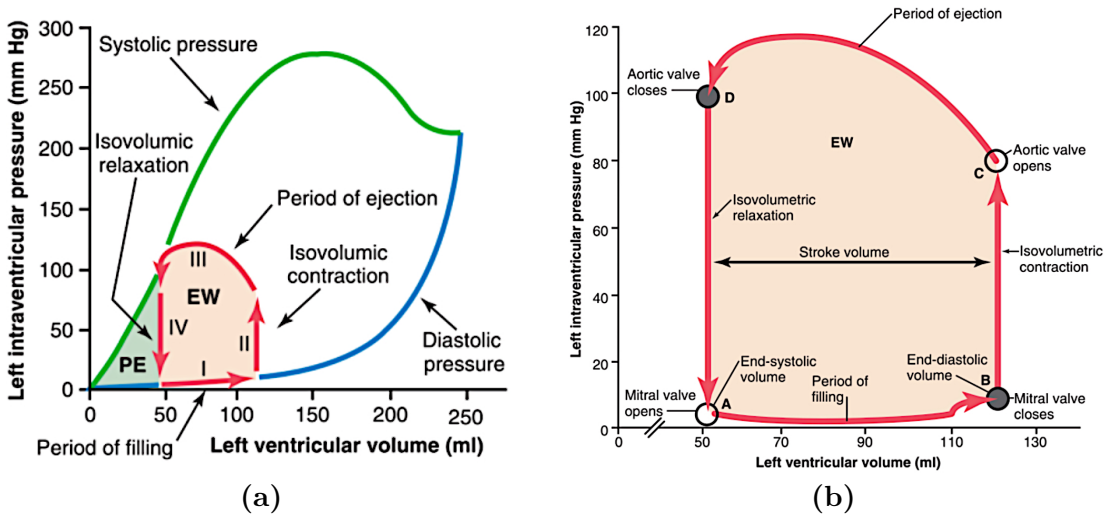

Figure 2.4: (a) Working diagram of the left ventricle with the P-V diagram. (b) Close-up P-V diagram. [Hal16]

curves named *diastolic pressure* and *systolic pressure*. Diastolic pressure is defined as the lowest point of each pulse, in a relaxed state of the heart, whilst systolic pressure represents the highest point of each pulse, occuring while the heart is contracting and ejecting blood. [SLH11] The blue curve of Figure 2.4a, representing the diastolic pressure, is calculated by gradually filling the heart with higher blood volumes and then measuring the diastolic pressure just before ventricular contraction occurs. It is describing the heart's mechanical properties when the myocardium is in a relaxed state. The green curve in Figure 2.4a, named systolic pressure, is plotted by measuring the systolic pressure over varying filling volumes for constant ventricle volumes. The red lines in Figure 2.4a and Figure 2.4b indicate the cardiac cycle and its four action phases, as described above. The line between points A and B in Figure 2.4b depicts the period of rapid filling. The isovolumic contraction is represented by line II in Figure 2.4a, respectively between points B and C in Figure 2.4b. The ejection phase is depicted by III in Figure 2.4a and the line referred to as IV represents the period of isovolumic relaxation. The area of the work diagram, marked with EW in Figure 2.4 is a measure of the work done by the heart. The P-V diagram furthermore enables calculation of the Ejection Fraction (EF), which describes the percentage value of the ventricle volume ejected during systole. It is determined trough

$$EF = \frac{SV}{EDV} * 100. \tag{2.2}$$

For a healthy heart at rest, with a stroke volume of about $70\,ml$ and an EDV of about $110 - 120\,ml$, the EF is at about $50 - 60\,\%$. In cases of heart failure the EG can decrease to about $20 - 25\,\%$. Therefore, knowledge of the P-V diagram is an important prerequisite in understanding myocardial diseases. [SLH11]

2.2 Heart failure

The World Health Organization (WHO) lists cardiovascular diseases (CVDs) as the global number one cause of death. In 2016 about 17.9 million people died from CVDs, representing 31 % of all global death that year. [Wor20]
In case of heart failure, the heart is unable to provide the required amount of blood flow to the cardiovascular system in order to supply all organs and tissue with oxygen. Heart failure does not directly represent a disease but rather a clinical syndrome. Nevertheless, the symptoms of different forms of heart failure are very similar and eventually manifest themselves in a decreased cardiac output. One acute consequence of heart failure, for example, is the feeling of shortness of breath. In the long term, however, severe heart failure can also lead to muscle weakness and a lack of concentration.

According to Schmidt et al. [SLH11], heart failure can be attributed to either systolic dysfunction or diastolic dysfunction. Systolic dysfunction can manifest itself in several ways. One is a reduced contractility and stroke volume of the heart. Causes may be, for example, a coronary artery disease that limits ogxygen supply or a preceding myocardial infarction. Secondly, there may be increased pumping resistance due to an outflow obstruction. This may be the result of arterial hypertension, among other things. Furthermore, cardiac arrhythmias or a heart attack can lead to systolic dysfunction. Figure 2.5a displays the variation of the P-V diagram, comparing a normal functioning heart (dotted line) and one impaired by heart failure with a systolic dysfunction (solid line). In diastolic functional impairment, the dysfunction is evident in the course of the filling phase. This can be triggered, among other things, as a result of reduced compliance of the myocardium due to hypertrophy or fibrosis. The change in the P-V diagram for diastolic heart failure is illustrated in Figure 2.5b.

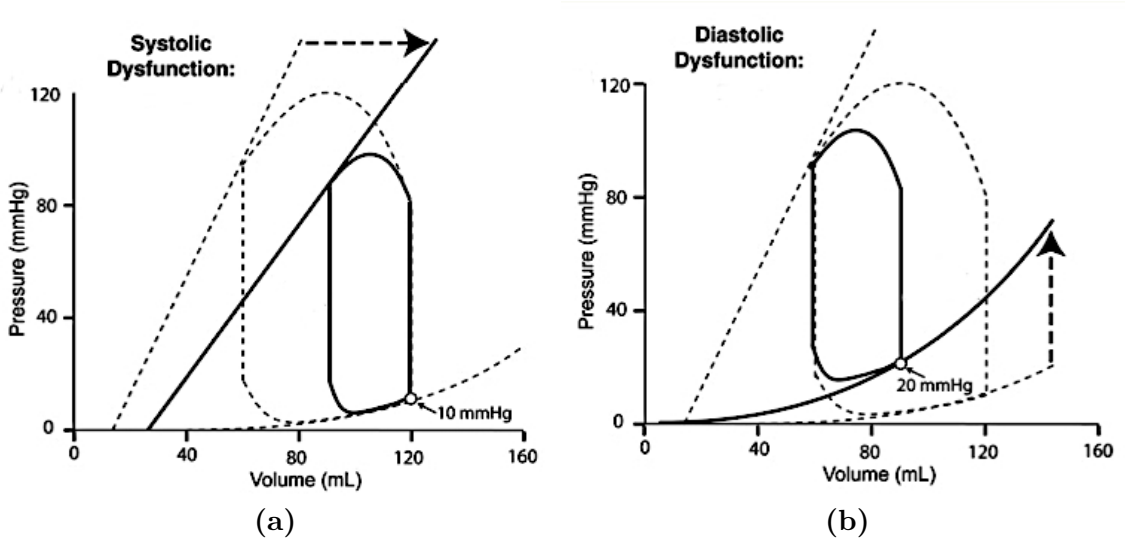

Figure 2.5: P-V diagram for heart failure in cases of (a) a systolic dysfunction and (b) a diastolic dysfunction according to [KR15]. The dotted lines symbolize normal heart function in comparison to the dysfunction represented by solid lines.

For treatment of heart failure, drug therapy using beta-blockers is initially targeted in most cases. However, if this is not successful, the use of ventricular assist devices can be a useful alternative in order to relieve the heart and provide sufficient blood flow. [SLH11]

2.3 Ventricular Assist Devices

Despite the fact that heart transplantation (HTx) still is the gold standard for treatment of patients with terminal heart failure [Sch10] ventricular assist devices (VADs), as a kind of mechanical circulatory support (MCS) technology, are becoming more and more important in treating patients with CVDs. There are two reasons for this. On the one hand, CVDs are gaining in importance due to demographic change. On the other hand, there is an increasing shortage of donor organs. [DMH19]

2.3.1 Therapeutic objective

Traditionally the therapeutic goals of VAD treatment can be divided into three categories: *bridging to transplantation* (BTT), *bridging to recovery* (BTR) and *destination therapy* (DT). However, in some cases also the classification into *bridging to decision* (BTD) and *bridging to transplantability* are mentioned as well. The decision for one of these goals is based on the type of CVD and the condition the patient is in when receiving VAD assistance. [KSS+11] In clinical praxis different classification techniques connecting the patient condition with the estimated survial time and the need for VAD assistance are used. An overview of the relation between the INTERMACS Score, the New York Heart Association(NYHA)-classification and the patient's condition is presented in Table 2.1. The INTERMACS Score, which is

INTERMACS Score	NYHA	Patient condition	Survival time
1	IV	critical cardiogenic shock	hours
2	IV	increasing catecholamine demand	days
3	IV	stable under inotropics	a week
4	IV	frequent decompensation	weeks-month
5	IV	rest discomfort/ not resilient	weeks-month
6	IV	rest discomfort/ merely resilient	month
7	IIIb	merely resilient	one year survival rate: 50-70%

Table 2.1: Relation between INTERMACS Score, NYHA-classification, patient condition and approximate survival time based on [Eif18].

based on data from patients which have received VAD treatment, links the need for a VAD and the appropriate time frame in which the device needs to be implanted. It is of high importance in the decision of the therapeutic objective for VAD treatment.

[DMH19]
The goal of *bridging to transplantation* has a big relevance with patients in NYHA-IV Stadium showing hemodynamical instability. Due to a heart transplantation being the desired final treatment for these patients, there must be no contraindication to HTx. In case the patient does show a contraindication, such as malignant tumors or an uncontrollable sepsis, the therapeutic objective changes from BTT to DT. In order for a treatment with a VAD as destination therapy being indicated all conservative treatment options need to be exhausted. Due to the ever-growing shortage of donor organs, DT as a therapeutic approach in patients with heart insufficiency will become more relevant in the future even in cases usually suited for heart transplantation. [DMH19] There may occur some cases in which at first a contraindication for HTx exists, which later on may dissolve. These indicate a therapy based on a *bridging to transplantability* goal. [KSS+11]
The indication for a *bridging to recovery* approach is twofold. Either the patient shows heart failure as a result of ischemia reperfusion damage or due to infectious genesis. In the first case the myocardium usually is able to recover within a few days, whereas in the second one the potential and the time necessary for recovery depend on how badly the tissue is damaged. In either scenario a weaning from the VAD is an essential part of therapy. [DMH19]
If a patient is admitted in cardiogenic shock and medical treatment is not sufficient, *bridging to decision* becomes a relevant form of therapy. By providing the patient with a VAD, a more accurate assessment of the patient's condition is possible. Based on this, the decision on further treatment can be thought through more thoroughly. [KSS+11]

2.3.2 Technology

Since the first artificial blood-pump has been implanted in 1963 [LHH+63] technology of VADs has improved significantly.
The general aim of ventricular assist devices is to provide mechanical support in pumping blood through the human body with the heart remaining inside the patients body. Despite there being several types of VADs, all of them are working according to the same principle. Blood is taken from the circulatory system through the pumps inlet and ejected at another location via the outlet of the pump. [LW16]

VADs are differentiated by three criteria: localization of the device inside the human body, flow profile and implantation strategy.
Regarding localization of the assistance device there are three types of VADs. With around 93 % of all implemented devices the most commonly used ones are the left ventricular assist devices (LVADs). [DMH19] LVADs are placed inside the left ven-

tricle, from where they are pumping blood into the aorta [GSL+03]. The second localization option is placing the device as support for the right ventricle. These devices are therefore called right ventricular assist devices (RVADs). RVADs are positioned in a way that blood is taken from the right atrium and ejected into the pulmonary artery. [DMH19] In some cases RVADs in combination with the aforementioned LVADs are used to build a biventricular assist device (BVAD). This type of heart support is mainly used for more severe heart diseases with a high risk of developing right heart failure. [SH19]
The flow profile as the second criterion for VAD distinction is represented by pulsatile and continuous flow devices. Assistance with pulsatile devices can either be implemented to support the heart in a counter pulsation approach, working synchronous to the heart cycle, or as an asynchronous support. The most commonly known type of pulsatile device is a pneumatically driven pump ventricle. [LW16] However, according to the Interagency Registry for Mechanically Assisted Circulatory Support (INTERMACS) over 95 % of all implanted devices are continuous flow devices [KPK+17]. These, in their most commonly used form, are electrically driven rotational blood pumps. A technological difficulty with these devices is the high probability of blood damage due to small gaps and very high rotational speed. In exchange for this problematic these devices enable a dynamic adaption to the patients physiological needs by being able to quickly adjust parameters like the motor current. The possibility of keeping track of these signal characteristics furthermore makes it possible to detect malfunctions such like misplacement of the pump. [LW16]
Implantation of the VADs can be performed in one of three ways: paracorporeal, intracorporeal or percutaneous [DMH19]. For VAD systems which follow a paracorporeal approach, only the in- and outflow cannulas are located inside the human body. The cannulas are connecting the pump located outside the body with the ventricle and the vessels. Due to the pump being placed outside of the patient's body, these systems provide the option for pediatric MCS. For most other systems this is not possible due to the device being to big to fit inside a child's body. [SBL19]
One example for paracorporeal systems are the aforementioned pneumatically driven pump ventricles [LW16]. In contrast to the paracorporeal devices, where the pump itself, as well as the control unit is situated outside the body, in percutaneous devices the pump is placed inside the body. The control unit however, remains outside the patient's body and is connected to the pump via leads. The intracorporeal devices are fully implanted into the body. [SBL19]
As far as the other two criteria for VAD differentiation are concerned, all combinations of localization and flow control are possible [SBL19]. As an example of a percutaneous device, [DMH19] names the Impella 2.5, which is a rotary blood pump with continuous flow used for left ventricular assistance.
The proportions of different VAD types and therapeutic goals are illustrated in Table 2.2 based on the International Mechanically Assisted Circulatory Support (IMACS) register.

VAD type		Therapeutic objective	
LVAD	93%	DT	40%
BVAD	4%	BTD	30%
TAH	2%	BTT	29%
unknown	0.1%	others (BTR, ...)	1%
RVAD	0.05%		

Table 2.2: Percentages of VAD types and therapeutic objectives in mechanical heart support based on [DMH19].

3 Control Theory

Since this thesis addresses the implementation of flow control algorithms for a left ventricular assist device, this section will focus on the fundamentals of notation and structure of a standard control loop. Furthermore, the basic principles of PI-controllers and iterative learning control (ILC) are discussed, since these are used within the practical part of the thesis.

3.1 Fundamentals

The basic task of control engineering is to influence a time-varying process from the outside with the goal of executing the process in a predetermined manner. A control system is characterized in particular by the feedback of the controlled variable to the reference variable. The reference variable comprises the state that has to be achieved. In theory, this is represented by a control loop with the components shown in Figure 3.1. The plant $G(s)$ transfers the actuating variable $u(t)$, as well as the influence of the the disturbance $d(t)$, to the controlled variable $y(t)$. This variable is permanently compared with the reference variable $w(t)$ by means of a feedback loop, providing the control error

$$e(t) = w(t) - y(t). \tag{3.1}$$

The controller $G_c(s)$ then transfers the control error to the actuating variable again. The aim of the control loop is to achieve the smallest possible control error with the highest possible damping. Since these goals contradict each other, a trade off must always be accepted here. [ZR17]
However, there are some general requirements for the closed control loop which have to be fulfilled. The first requirement states that the closed loop needs to be stable, which is met if the control loop responds to a finite excitation with a finite output signal. The second condition is the requirement for disturbance rejection, stating

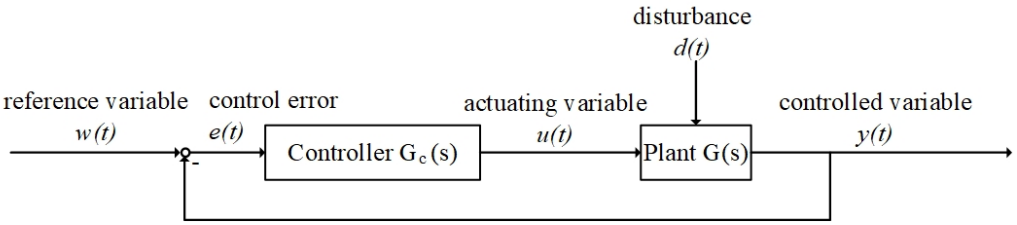

Figure 3.1: General structure of a control loop

that the controlled variable needs to follow the reference variable asymptotically, so that

$$\lim_{t\to\infty} e(t) = 0. \tag{3.2}$$

Another requirement is that the dynamic relationship between the reference variable $w(t)$ and the controlled variable $y(t)$ must satisfy specified quality requirements. The last requirement states that the first three requirements must be satisfied despite uncertainties in the plant, being called robustness requirement. More detailed information on these requirements can be found in [Lun10].

The plant $G(s)$ corresponds to the part of the system in which the physical quantity to be controlled is influenced by the controller. The calculation of the plant by setting up and solving differential equations, is possible only in a few cases. Due to this, the determination of the plant's characteristic values is usually carried out experimentally. There are several basic types of plants, classified according to their dynamic behavior. As only the PT_1-element is used in the practical part of this thesis, all other variations will not be discussed at this point. Detailed information on this topic can, once more, be found in [Lun10].
The PT_1-element is the plant type which is most common in technical equipment. A PT_n-element in its static state reacts proportionally to the input value and has a distinct transition behavior. The index n describes the order of the system. Therefore, a PT_1-element is a proportional delay element of first order. The mathematical formulation of the transfer function of a PT_1-element is

$$G(s) = \frac{k_s}{1 + sT}. \tag{3.3}$$

The value k_s describes the static gain, which equals the final value of the transfer function. The time constant T enables an impression of the speed with which the system can react to changes at the input. It is defined as the time at which the transfer function reaches 63 % of its static gain. [Lun10] Figure 3.2 shows the transfer function of a PT_1-element and its significant parameters.

3.2 PI-controller

A PI-controller is a control structure commonly used for linear systems. This structure consists of both a proportional (P) and an integral (I) control element. The output value of a P-controller is proportional to its input value. In relation to the control loop in Figure 3.1 this leads to

$$u(t) = K_P e(t). \tag{3.4}$$

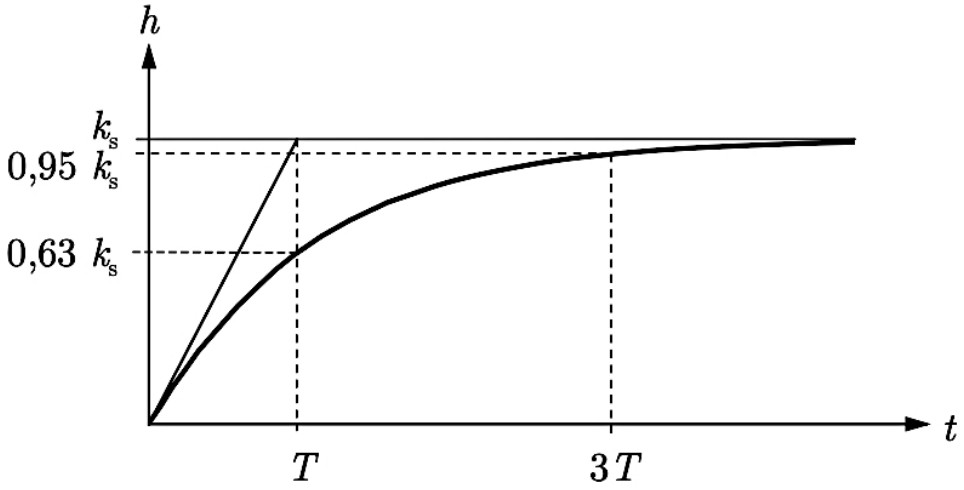

Figure 3.2: Transfer function of a PT_1-element [Lun10].

Using Laplace transformation the transfer function for a P-controller can be determined as

$$G(s) = \frac{u(s)}{e(s)} = K_P. \tag{3.5}$$

Therefore, the step response of this controller equals a step weighted with the Parameter K_P.
The relationship between input and output value of an I-controller is described through

$$u(t) = K_I \int e(t)dt. \tag{3.6}$$

Just as for the P-controller, Laplace transformation can be used to determine the transfer function of the I-controller. This leads to

$$G(s) = \frac{u(s)}{e(s)} = \frac{K_I}{s}, \tag{3.7}$$

which indicates a step response in form of a ramp with slope K_I. In order to generate a PI-controller these element from (3.4) and (3.6) can be added, which leads to

$$u(t) = K_P e(t) + K_I \int e(t)dt. \tag{3.8}$$

The Laplace transformation can be used again to compute the transfer function

$$G(s) = \frac{u(s)}{e(s)} = K_P + \frac{K_I}{s}. \tag{3.9}$$

The step response of the PI-controller, illustrated in Figure 3.3, shows both the weigthed step from the P-controller and the ramp from the I-controller.

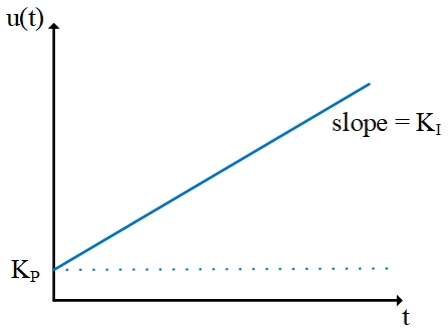

Figure 3.3: Step response of a PI-Controller

3.2.1 Tuning rules

In regard to the controller parameters, tuning is of great importance. If the parameters are chosen incorrectly it can lead to unstable system behavior, which may result in system damage. There are many different approaches to tuning a PI-Controller in order to achieve the best system performance. These range from heuristic methods over analysis of pole-zero plots to computer-aided numerical parameter optimization. [Lun10] At this point the tuning rules according to Ziegler Nichols (ZN) and the rules according to Chien Hrones Reswick (CHR) will be discussed, as these are used for the implementation of flow control in the practical work. Information on other approaches can be found in [AHR11].

Tuning rules according to Ziegler Nichols

The tuning rules according to Ziegler Nichols are one of the most commonly used heuristic methods in tuning controller parameters for PI-controllers. They are used especially if a mathematical model of the plant is not available but the plant can be approximated as a PT_n-element. [ZR17] A necessary condition for this is the need of being able to experimentally identify the step response of the plant without risk of damage to the system. After the step response has been determined it is displayed graphically. Then the inflection tangent is drawn into the step response as shown in Figure 3.4. The blue line represents the step response, the red line the inflection tangent, respectively. The gain K_S, the delay time T_v and the settling time T_g can be read from the graph. With these the factor K_P is calculated as

$$K_P = \frac{T_g}{K_S T_v}. \tag{3.10}$$

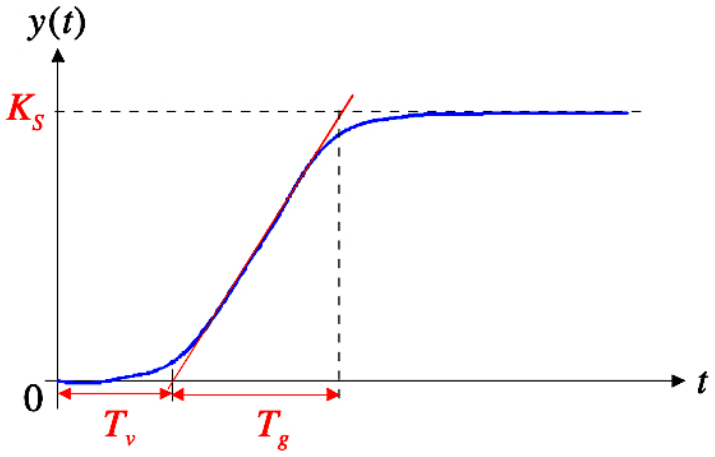

Figure 3.4: Inflection tangent method for Ziegler Nichols and Chien Hrones Reswick

The factor K_I is calculated according to:

$$K_I = \frac{K_P}{T_N}, \tag{3.11}$$

with

$$T_N = 3.33 T_v. \tag{3.12}$$

Tuning rules according to Chien Hrones Reswick

The tuning method according to Chien Hrones Reswick is very similar to the one by Ziegler Nichols. However, this method provides the ability to adjust the transient response of the control loop. The tuning parameters can either be chosen in a way to provide an over damped behavior or a course providing 20 % overshoot. [AHR11] For both options the step response and its inflection tangent are graphically displayed, as for the Ziegler Nichols approach in Figure 3.4. The values for K_S, T_v and T_g can be read from the plot. The parameter value K_I again is calculated following (3.11). the formulas for calculatio of K_P, T_N and T_D are given in Table 3.1.

3.3 Iterative Learning Control

The use of iterative learning control aims to improve control performance for systems which execute the same task repeatedly under constant operation conditions. This

over damped		20% overshoot	
K_P	T_N	K_P	T_N
$0.35\frac{T_g}{K_S T_v}$	$1.2T_v$	$0.6\frac{T_g}{K_S T_v}$	T_v

Table 3.1: Tuning parameters according to Chien Hrones Reswick

improvement is based on the idea that it is possible to include error information from previous iterations into the adjustment of the actuation variable during the current iteration. The standard control structure of an ILC algorithm is presented in Figure 3.5. Considering a linear-time-invariant single-input-single-output system,

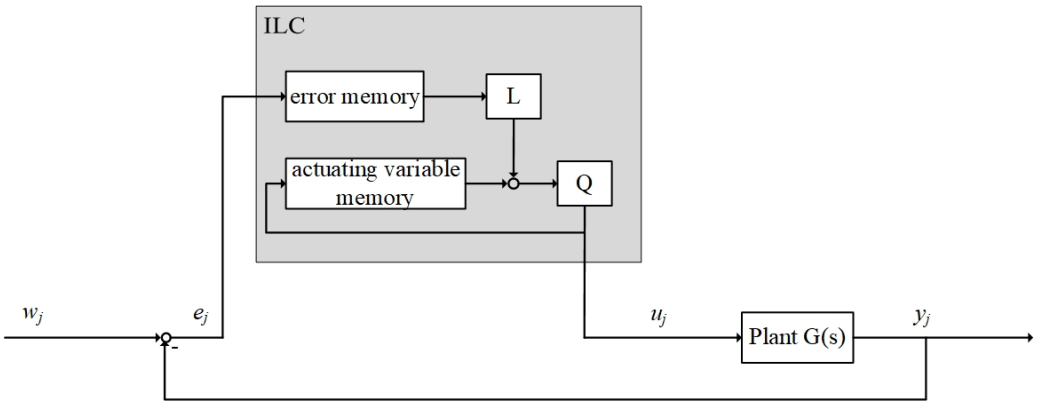

Figure 3.5: Standard ILC control loop

the ILC learning algorithm would be as follows:

$$u_{j+1} = Q(q)[u_j(k) + L(q)e_j(k+1)] \tag{3.13}$$

where k is the time index, j is the iteration index, $Q(q)$ is defined as the Q-Filter and $L(q)$ represents the learning function. The performance error signal e_j is defined as

$$e_j = w_j - y_j. \tag{3.14}$$

Feedback controllers, such as PI-controllers, are only able to include the current changes in control error. By taking into account the information from previous iterations, low tracking errors are achievable through an ILC. This results in very high performance with convergence during the first few iterations. This can be achieved even for systems prone to repeating disturbances and model uncertainties. While feedback control has a lag in transient tracking due to reacting to inputs and disturbances, ILC, as a feedforward controller, does not. Another advantage of ILC use is that there is no need for disturbances to be known or measured, as long as

these signals show repeating behavior during each iteration. Furthermore, by storing signal information during each iteration, ILC enables advanced filtering and signal processing of the control error. However, ILC utilization holds some issues in regard to non-repeating disturbances or noise influences. In these cases it may be useful to combine ILC approaches with a feeback controller. A combination of the systems is also recommended if the behavior of the plant is not stable. [BTA06] A parallel architecture of a feedback controller in combination with an ILC is illustrated in Figure 3.6.

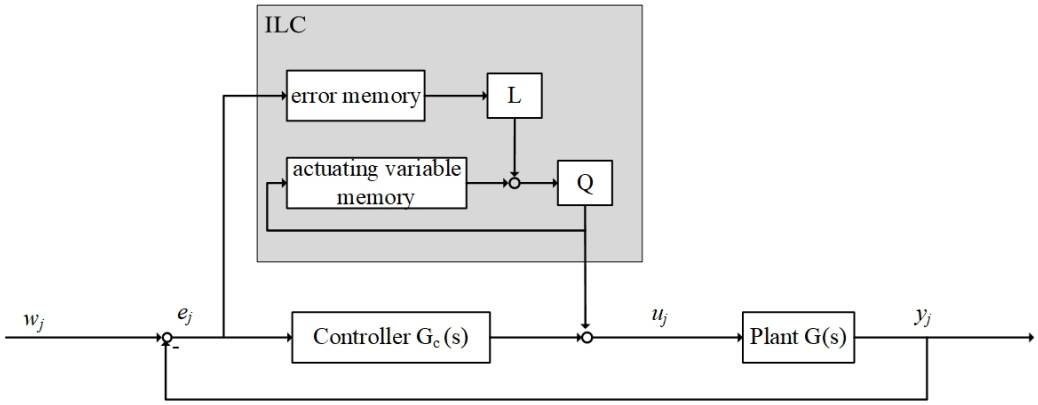

Figure 3.6: Parallel architecture of ILC with feedback controller

There are several approaches to designing an ILC. In general, an ILC ideally learns only the repeating disturbance patterns without being influenced by noise. The most common types of ILC learning functions are the P-, D- and PD-type learning functions. As an ILC does have an natural integrator action from one iteration to the next, I-type learning functions are not used that frequently.
The discrete-time learning function for a standard PD-type ILC is given as either

$$u_{j+1}(k) = u_j(k) + k_p e_j(k+1) + k_d[e_j(k+1) - e_j(k)] \tag{3.15}$$

or

$$u_{j+1}(k) = u_j(k) + k_p e_j(k) + k_d[e_j(k+1) - e_j(k)]. \tag{3.16}$$

k_p represents the proportional gain while k_d is the derivative gain. In case a P-type learning function is implemented the derivation gain is set to $k_d = 0$. For a D-type learning function $k_p = 0$ is used, respectively.
The performance of these ILC types depends mainly on accurate parameter tuning and does not require an accurate mathematical model of the plant. Despite these approaches being frequently used, there are no tuning guidelines similar to the ones mentioned for PI-controller tuning. However, a commonly used way to influence the process behavior is to modify the learning algorithm to include a Q-Filter. This filter can be used to disable learning at high frequiencies in order to filter high-frequency noise. It furthermore increases robustness. First a filter type, such as

Butterworth or Chebyshev, is specified. The bandwith can then be interpreted as a tuning parameter in addition to the proportional gain k_p. Initially learning gain and filter bandwidth are set to low values. When a steady baseline behavior and error performance is achieved, the parameter values can be increased to improve performance. The learning gain influences the rate of error convergence while the Q-Filter influences the error performance. The higher the filter bandwidth the more increased the performance. However, this includes a trade-off in robustness. For lower filter bandwidth high robustness can be achieved in a trade-off in performance. Besides the P-,D- and PD-type ILC there are other design approaches. The H_∞ method can be used to design a robustly convergent ILC controller, with a trade-off in performance. A quickly converging ILC approach can be achieved by using the plant inversion method. This however depends on an accurate modeling of the plant. The quadratically optimal ILC approach uses quadratic performance criteria to design an optimal ILC. Further information on these alternative design methods is provided in [BTA06].

4 Identification

4.1 Sputnik VAD

The Sputnik VAD is an axial-flow blood pump, developed in a cooperative project of the National Research University of Electronic Technology, OJSC Zelenograd Innovation-Technology Center of Medical Equipment, FSBI "Academician V.I. Shumakov Federal Research Center of Transplantology and Artificial Organs", Ministry of Health of Russian Federation, DONA-M LLC and BIOSOFT-M LLC in 2009. [ST15]
This device is used for left ventricular assistance in patients with acute heart failure. The therapeutic objective in implantation of a Sputnik VAD is bridging to transplantation. The VAD is able to pump up to 10 liters of blood per minute with a continuous flow profile. The implantable pump weighs about 200 g, has a length of 81 mm and a maximum diameter of $34\,mm$. It consists of a moving and a stationary part. The moving part, the impeller, which is a rotor with four blades, contains a permanent NdFeB-magnet which is actuated by a brushless DC motor. The rotor spins clockwise with speed values between $4000 - 10000\,rpm$. An overview of the pumps specification is presented in Table 4.1. The stator is located inside a tita-

Blood flow	0-10 L/min
Rotational speed	4000-10000 rpm
Length	81 mm
Diameter	34 mm
Weight	200 g

Table 4.1: Specifications of Sputnik VAD

nium housing with a $16\,mm$ diameter. The stationary part of the pump consists of a flow straightener with three stationary blades and a flow diffusor with three twisted blades. The flow straightener is located in front of the rotor and straightens the incoming blood flow into the rotor. Behind the rotor the blood is directed into the diffusor. Figure 4.1 depicts a cross-section of the Sputnik VAD and identifies its individual components. The connection between the pump and the cardiovascular system is performed using in- and outflow cannulas, a felt ferule and vascular prosthesis which is sewed to the aorta. [ST15] The Sputnik VAD is powered using two lithium-ion batteries, fully loaded providing enough energy for up to eight hours of system support. The maximum charging time for the batteries is less than five hours. During this time the batteries can either be exchanged by another set of

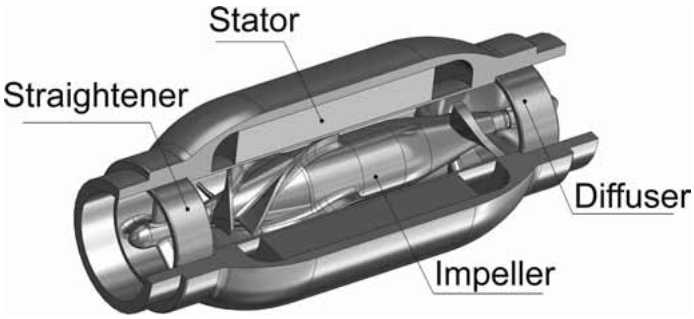

Figure 4.1: Cross-section of the Sputnik VAD [ST16]

batteries or the system can be powered through connection to an AC network. A microprocessor-based driving unit is used to regulate the pump speed, manage the power supply and store parameter data. It is connected percutaneously to the pump with an up to 170 cm long and 5 cm wide lead. [ST15]
During the practical part of this work the pump was controlled using the servo controller module ESCON 50/4 EC-S from maxon motor. This is a 4-quadrant pulse width modulation controller for controlling motors without Hall sensors.

4.2 Hardware in the Loop Test Bench

For all measurements and tests performed during this thesis, a hardware in the loop (HiL) test bench of the Chair of Medical Information Technology at RWTH Aachen University was used. The test bench is implemented as a feedback controlled human circulatory system simulator. With the aid of the test rig, it is possible to test MCS systems under various physiological and pathological load patterns of the heart.
The structure of the mock circulatory loop (MCL) is depicted in Figure 4.2. The boxes marked as V_1 and V_2 are pressure compartments simulating the volume of the left ventricle and the aorta, respectively. Therefore, the pressure values of these compartments referred to as p_1 and p_2 can be physiologically compared to the pressure values of the left ventricle and aorta. The MCL is actuated by three gear pumps (GP_1, GP_{12} and GP_2) and two voice coil actuators (VCA_1 and VCA_2). The Sputnik VAD is connected in parallel to the pressure chambers, enabeling tests similar to real use case. This way, the VAD can be subjected to similar pressure changes in the differential pressure between the aorta and ventricle as would be the case when used on the beating heart.
By controlling the MCL through a dSpace system (DS1103), pressure in the chambers can be adjusted in real time to simulate different cardiac dysfunctions. The dSpace system furthermore enables recording of reference signal presented to the MCL as

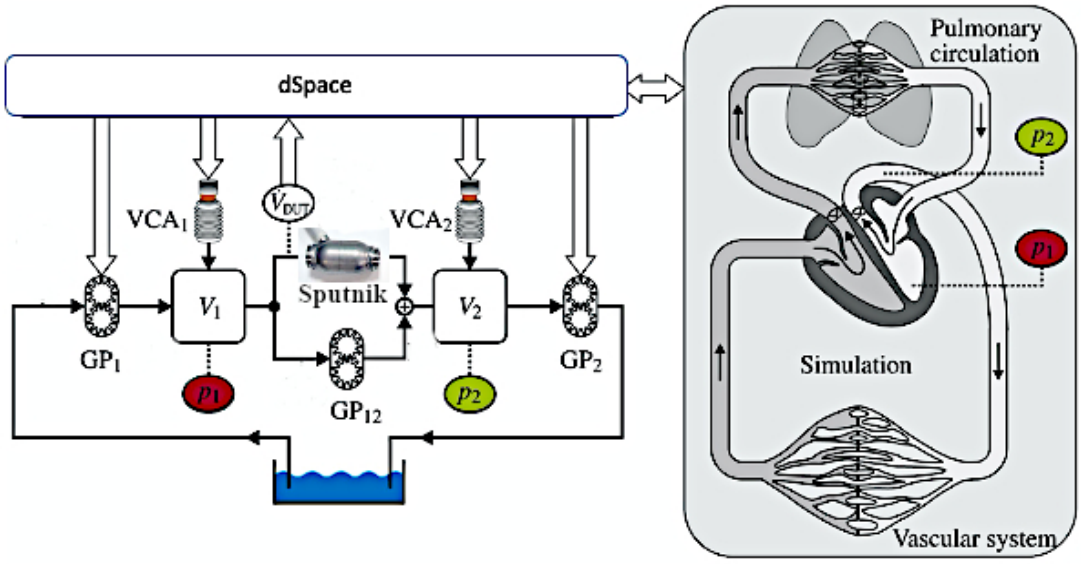

Figure 4.2: Structure of the HiL human ciculatory system simulator based on [MRS+15]

well as real time measurements. All recorded data can be exported formatted as Matlab matrices.
As the Sputnik VAD is not regularly included into the MCL setup, flow through the device can not be measured without further equipment. For this purpose the Transonic Systems Inc. T110 flow-meter is included in the setup. The flow sensor measurement is based on ultrasonic technology. The sensor probe is adjusted onto the tube leading from the pressure chamber representing the left ventricle to the VAD. The flow-meter as well is connected to the dSpace system, enabling recording of the measured flow values. In Figure 4.2 these values are represented by $\dot{V}_{DUT}$.
The ESCON servo controller mentioned in chapter 4.1 is also connected to the dSpace system. Using the digital input port of the controller a set value for regulation of the rotational speed can be transferred to the controller after setting the value in the system.
The dSpace system itself is controlled with the use of the program ControlDesk. This software provides the oportunity to include matlab and simulink source code. By this controllers designed under use of Simulink can directly be tested at the HiL test bench.

4.3 System Identification

5 Flow Control

During this chapter implementation and evaluation of various control algorithms for flow control purposes will be presented.

5.1 Controller Design

5.1.1 PI Controller

Chien Hrones Reswick

5.1.2 Iterative Learning Control

5.1.3 Iterative Learning Control with varying iteration length

5.2 Evaluation

5.2.1 PI Controller

Chien Hrones Reswick

5.2.2 Iterative Learning Control

5.2.3 Iterative Learning Control with varying iteration length

6 Conclusion and future work

Using current iteration learning control (ILC2 s.99)

Higher-order learning algorithms (ILC2 s98)

A Appendix

Bibliography

[AHR11] Arora, Ashish ; Hote, Yogesh V. ; Rastogi, Mahima: Design of PID Controller for Unstable System. In: Balasubramaniam, P. (Hrsg.): *Control, Computation and Information Systems*. Berlin, Heidelberg : Springer Berlin Heidelberg, 2011. – ISBN 978–3–642–19263–0, S. 19–26

[BTA06] Bristow, D.A. ; Tharayil, M ; Alleyne, A.G.: A survey of iterative learning. In: *Control Systems, IEEE* 26 (2006), 07, S. 96 – 114. http://dx.doi.org/10.1109/MCS.2006.1636313. – DOI 10.1109/MCS.2006.1636313

[DMH19] Dashkevich, A ; Michel, S ; Hagl, C: Indikationsstellung und Therapieziele der mechanischen Kreislaufunterstützung. In: *Medizinische Klinik-Intensivmedizin und Notfallmedizin* 114 (2019), Nr. 5, S. 452–458

[Eif18] Eifert, S: Perkutane und chirurgische Optionen der mechanischen Kreislaufunterstützung in der Therapie der terminalen Herzinsuffizienz. In: *Der Anaesthesist* 67 (2018), Nr. 5, S. 321–325

[GSL+03] Grabellus, F. ; Schmid, C. ; Levkau, B. ; Stypmann, J. ; Scheld, H. ; Baba, Hideo A.: Myokardiale Veränderungen unter mechanischer linksventrikulärer Unterstützungstherapie. In: *Der Pathologe* 24 (2003), Nr. 2, S. 83–90

[Hal16] Hall, John E.: *Guyton and Hall Textbook of Medical Physiology, Jordanian Edition E-Book*. Elsevier, 2016

[KPK+17] Kirklin, James K. ; Pagani, Francis D. ; Kormos, Robert L. ; Stevenson, Lynne W. ; Blume, Elizabeth D. ; Myers, Susan L. ; Miller, Marissa A. ; Baldwin, J. T. ; Young, James B. ; Naftel, David C.: Eighth annual INTERMACS report: Special focus on framing the impact of adverse events. In: *The Journal of Heart and Lung Transplantation* 36 (2017), 2020/08/05, Nr. 10, S. 1080–1086

[KR15] Katz, Arnold M. ; Rolett, Ellis L.: Heart failure: when form fails to follow function. In: *European Heart Journal* 37 (2015), 10, Nr. 5, 449-454. http://dx.doi.org/10.1093/eurheartj/ehv548. – DOI 10.1093/eurheartj/ehv548. – ISSN 0195–668X

[KSS+11] Krabatsch, T ; Schweiger, M ; Stepanenko, A ; Drews, T ; Potapov, E ; Pasic, M ; Weng, Y ; Huebler, M ; Hetzer, R: Fortschritte bei implantierbaren mechanischen Kreislaufunterstüzungssystemen. In: *Herz* 36 (2011), Nr. 7, S. 622

[LHH+63] Liotta, Domingo ; Hall, C.William ; Henly, Walter S. ; Cooley, Denton A. ; Crawford, E.Stanley ; DeBakey, Michael E.: Prolonged assisted circulation during and after cardiac or aortic surgery: Prolonged partial left ventricular bypass by means of intracorporeal circulation. In: *The American Journal of Cardiology* 12 (1963), Nr. 3, S. 399 – 405. – ISSN 0002–9149. – Symposium on Cardiovascular-Pulmonary Problems Before and After Surgery Part I

[Lun10] Lunze, Jan: Berlin, Heidelberg : Springer Berlin Heidelberg, 2010. http://dx.doi.org/10.1007/978-3-642-13808-9_1. http://dx.doi.org/10.1007/978-3-642-13808-9_1. – ISBN 978–3–642–13808–9

[LW16] *Kapitel* Herzunterstützungssysteme. In: Leonhardt, Steffen ; Walter, Marian: *Medizintechnische Systeme: Physiologische Grundlagen, Gerätetechnik und automatisierte Therapieführung*. Berlin, Heidelberg : Springer Berlin Heidelberg, 2016. – ISBN 978–3–642–41239–4, S. 107–144

[MRS+15] Misgeld, Berno J. ; RÃ¼schen, Daniel ; Schwandtner, Sebastian ; Heinke, Stefanie ; Walter, Marian ; Leonhardt, Steffen: Robust decentralised control of a hydrodynamic human circulatory system simulator. In: *Biomedical Signal Processing and Control* 20 (2015), 35 - 44. http://dx.doi.org/https://doi.org/10.1016/j.bspc.2015.04.004. – DOI https://doi.org/10.1016/j.bspc.2015.04.004. – ISSN 1746–8094

[SBL19] Sponga, Sandro ; Benedetti, Giovanni ; Livi, Ugolino: Short-term mechanical circulatory support as bridge to heart transplantation: paracorporeal ventricular assist device as alternative to extracorporeal life support. In: *Annals of cardiothoracic surgery* 8 (2019), 01, Nr. 1, S. 143–150

[Sch10] Schüller, Annika: Das Kunstherz – Möglichkeiten der mechanischen Kreislaufunterstützung (VAD). In: *intensiv* 18 (2010), Nr. 03, S. 138–147

[SH19] Shehab, Sajad ; Hayward, Christopher S.: Choosing Between Left Ventricular Assist Devices and Biventricular Assist Devices. In: *Cardiac failure review* 5 (2019), 02, Nr. 1, S. 19–23

[SK07] Schiebler, Theodor H. ; Korf, Horst-W: *Anatomie: Histologie, Entwicklungsgeschichte, makroskopische und mikroskopische Anatomie, Topographie*. Springer-Verlag, 2007

[SLH11] Schmidt, Robert F. ; Lang, Florian ; Heckmann, Manfred: *Physiologie des Menschen mit Pathophysiologie*. Springer-Verlag, 2011

[ST15] Selishchev, Sergey ; Telyshev, Dmitry: Ventricular assist device Sputnik: Description, technical features and characteristics. In: *Trends in Biomaterials and Artificial Organs* 29 (2015), Nr. 3, S. 207–210

[ST16] Selishchev, Sergey ; Telyshev, Dmitry: Optimisation of the Sputnik-VAD design. In: *The International journal of artificial organs* 39 (2016), 09. http://dx.doi.org/10.5301/ijao.5000518. – DOI 10.5301/ijao.5000518

[Wor20] World Health Organization: *Cardiovascular diseases (CVDs)*. https://www.who.int/news-room/fact-sheets/detail/cardiovascular-diseases-(cvds), Zuletzt besucht am 06.08.2020

[ZR17] Zacher, Serge ; Reuter, Manfred: *Regelungstechnik für Ingenieure: Analyse, Simulation und Entwurf von Regelkreisen*. Wiesbaden : Springer Fachmedien Wiesbaden, 2017. http://dx.doi.org/10.1007/978-3-658-17632-7_3. http://dx.doi.org/10.1007/978-3-658-17632-7_3. – ISBN 978–3–658–17632–7